nature communications

Article

https://doi.org/10.1038/s41467-024-54084-6

Robust bendable thermoelectric generators enabled by elasticity strengthening

Received: 8 August 2024

Accepted: 31 October 2024

Published online: 11 November 2024

Check for updates

Wenjun Ding[1], Xinyi Shen[1], Min Jin[2], Yixin Hu[1], Zhiwei Chen[1], Erchao Meng[3], Jun Luo[1] ✉, Wen Li[1] ✉ & Yanzhong Pei[1] ✉

Using body heat for instance, thermoelectric generators have promising applications for driving wearable electronics continuously but remain a challenge in terms of recoverable flexibility, as known highly-performing thermoelectrics are usually inorganics showing rigidity. It is conceptualized in this work a large elastic strain ensuring both a largely-curved recoverable bending and a full recoverability in thermoelectric performance after enormous bendings. This leads the current work to focus on a microstructure engineering approach for strengthening the elasticity of Ag_2Se, in which dense dislocations and refined grain induced by a multi-pass hot-rolling technique enable a significant enhancement in elasticity. The resultant hot-rolled elastic thin thermoelectric generators realize a record bendability, for at least 1,000,000 times at a tiny bending radius of 3 mm with an extraordinary power density. Such a bendability is applicable to the most curved surfaces of a human body, suggesting a promising strategy for powerful wearable thermoelectrics of all inorganics.

With the rapid development of portable electronics, a powerful, flexible, and durative power supply is urgently demanded. A direct generation of electricity using body or environmental heat by thermoelectricity provides a sustainable solution to this demand, in addition to the technical merits of safety, silence, reliability, and operation under all weather conditions[1,2].

A high power output is the primary criteria for practical thermoelectric generators, which is determined by the thermoelectric power factor ($PF = S^2/\rho$) with S and ρ being the Seebeck coefficient and resistivity, respectively. Many successful strategies offered guidelines for advancing thermoelectrics power factor[3–9]. These strategies, however, generally built upon the periodicity of atomic arrangements, which are usually limited in inorganic components that are typically rigid. This leaves the key challenge for wearable demands to make powerful thermoelectrics flexible since known inherently flexible organic and their composites are much inferior in performance[10–13]. Reported works on flexible thermoelectrics exhibit limited flexibility, with no safe bending times >1000 so far[14–18].

Many studies[19–22] on making thermoelectrics flexible were motivated by plasticity/ductility, which indeed ensured a large flexibility of no breakage. However, this may unsecure the recoverability of thermoelectric performance, since any irreversible atomic reconstructions due to plastic deformations lead to unrecoverable electronic and thermal transport properties.

Mechanically, elastic bendability offers a solution for fully recoverable flexible thermoelectrics, because it not only ensures safely permitted strains free of plasticity and breakages but also enables the reservation of initial functionalities after bendings. The maximum elastic strain (ε_E^{max}) is then the key material property measuring both recoverable bendability and recoverable thermoelectric performance, an enhancement of which is fundamentally needed for advancing flexible inorganic thermoelectric generators.

Intrinsic ε_E^{max} of a material is proportional to the Poisson's ratio (υ) via $\varepsilon_E^{max} \propto 1/(1-\upsilon)$[23], since a large υ enables a large corresponding transverse stress to help energy consumption under a longitudinal stress. This suggests a guidance for the selection of thermoelectric

[1]Interdisciplinary Materials Research Center, School of Materials Science and Engineering, Tongji University, Shanghai, China. [2]College of Materials, Shanghai Dianji University, Shanghai, China. [3]School of Materials Science and Engineering, University of Science and Technology Beijing, Beijing, China.
✉e-mail: junluo@tongji.edu.cn; liwen@tongji.edu.cn; yanzhong@tongji.edu.cn

materials having a large υ for flexible applications. Extrinsic factors further enabling a ε_E^{max}-enhancement can be often realized by refining grains and creating dislocations[24], indicating the commonly used strategy in metals[25–27] and ceramics[28,29] of plastic processing as an effective pathway for advancing flexible inorganic thermoelectrics.

Results and discussion

These motive the current work to focus on Ag_2Se foils for robust flexible thermoelectric applications, not only intrinsically due to its largest υ among inorganic thermoelectrics (Fig. S1 and Table S1), but also because of its plasticity allowing plastic processing for extrinsic dislocation creation and grain refinement. Surely, the highest thermoelectric power factor secured in Ag_2Se[30] among silver chalcogenides[31,32] guarantees its highest power output. Existing works on flexible Ag_2Se-based thermoelectric generators largely comes from the involvement of flexible organic components as either substrates[2,14,15,18] or additions[19,33].

A multi-pass hot rolling technique is utilized in this work, leading to an impressive density of dislocations reaching $10^{14}\,m^{-2}$ with a Burger's vector along the [001] direction as well as refinement of the grains from hundreds of micrometers down to just twenty micrometers, as evidenced by the electron backscatter diffraction (EBSD) observations[34,35] (Figs. 1, S2). Both of them significantly enhance the elasticity of the obtained Ag_2Se foils. Eventually, the multi-pass hot-rolled device of 36 μm thick, a typical thickness for flexible thermoelectric generators[14–17,36], survives at least 1,000,000-time elastic bending at a tiny bending radius of ~3 mm, without observable degradations in the high power output reserved from bulks. Both the output power density and the bendability are significantly superior to that of reported flexible thermoelectric devices of polycrystals, allowing a full applicability of a human body.

Hot rolling is a well-established and cost-effective plastic processing technique, which allows a feasible approach to deform and thin inorganic thermoelectrics at appropriate temperatures. Ag_2Se undergoes an orthorhombic to cubic structural transition at 407 K upon

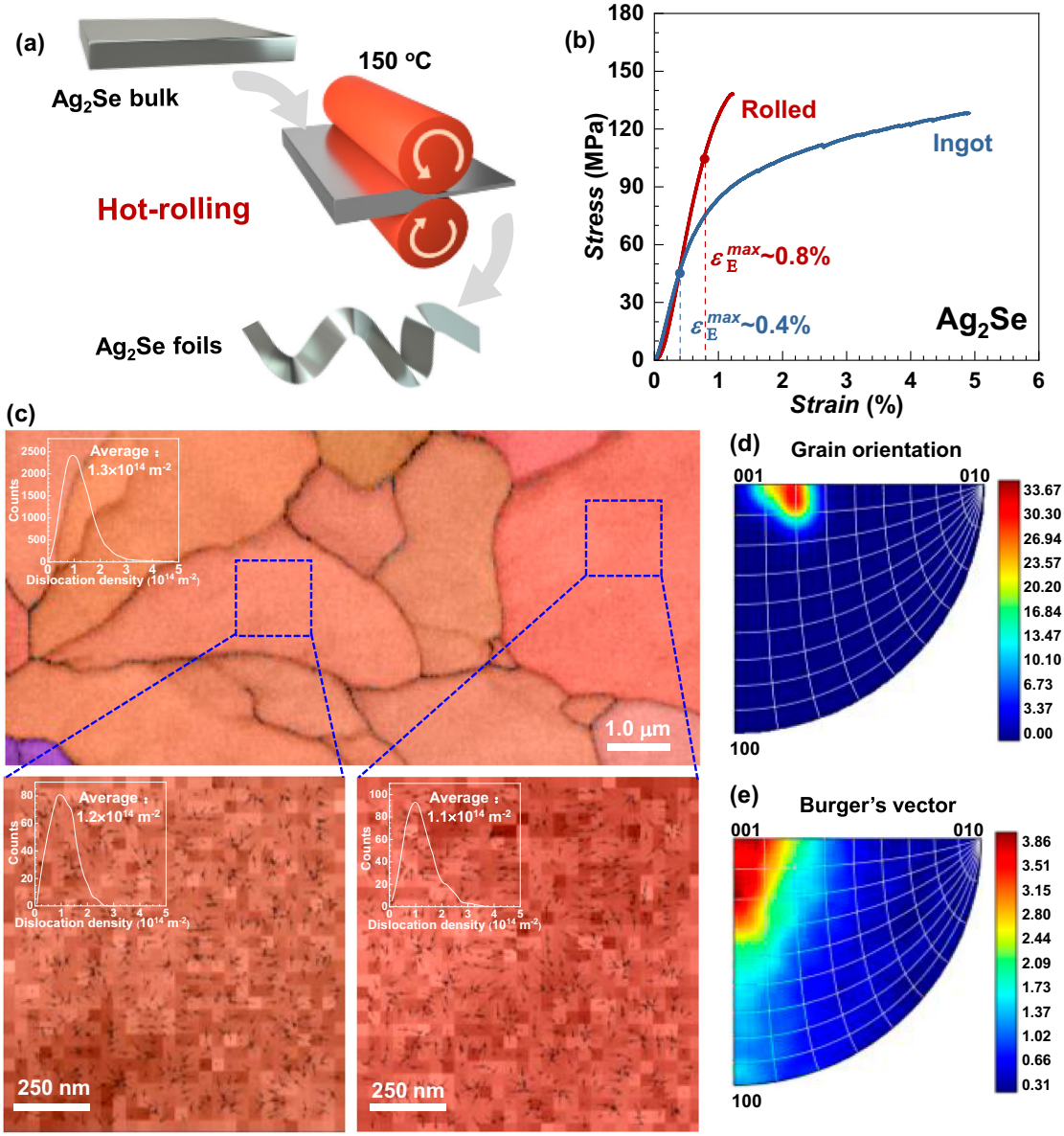

Fig. 1 | Fabrication, mechanical properties and microstructures. Schematic of hot-rolling process (**a**) for Ag_2Se foils. Stress versus strain of three-point bending test for Ag_2Se ingot and rolled foil (**b**). Electron back-scattering diffraction (EBSD) images and zoomed-in ones showing dense dislocations with statistic analyses in the rolled foil (**c**). The inverse pole figures show a [013] grain orientation (**d**) and a Burger's vector along [001] (**e**, black arrows).

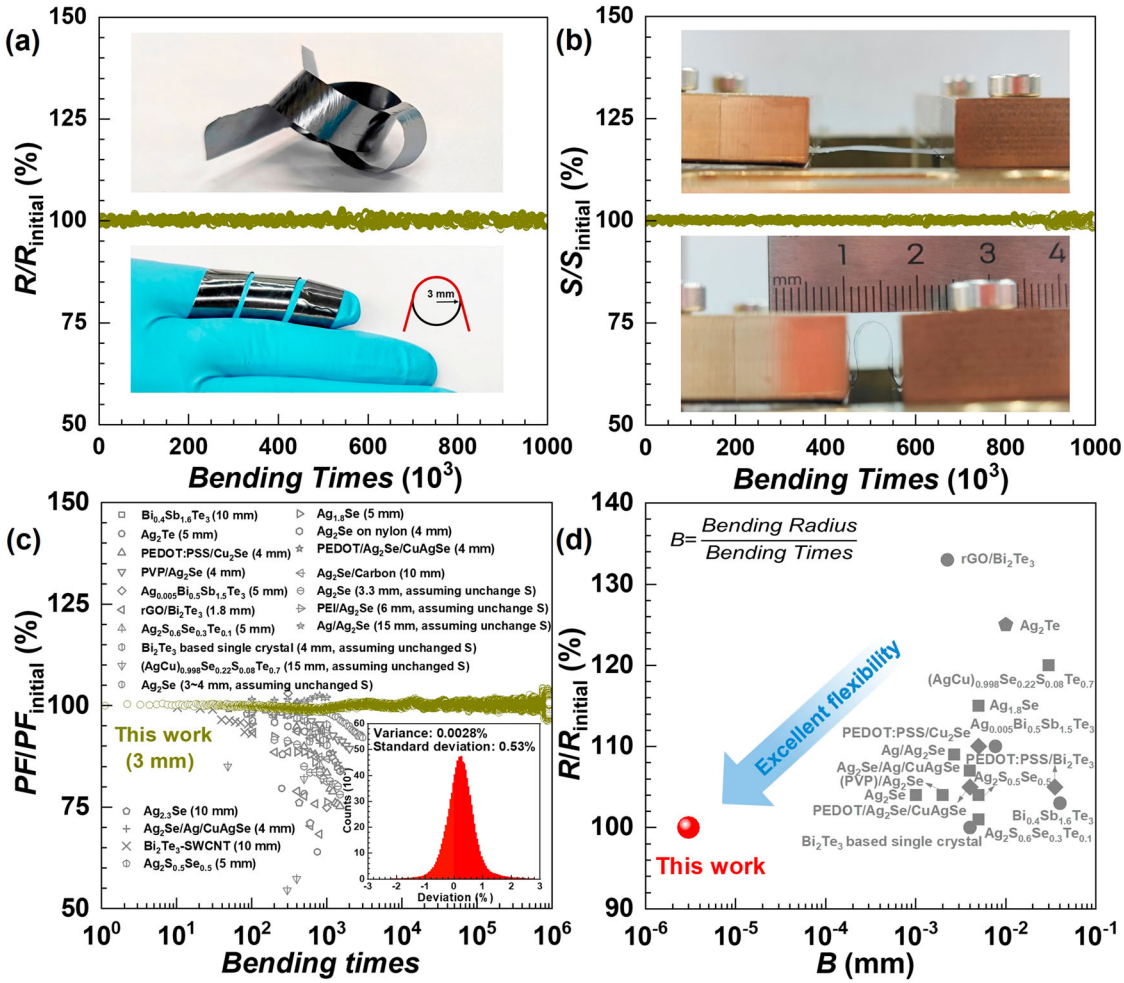

Fig. 2 | Bendability of hot-rolled thermoelectric Ag_2Se. The 36 μm thick device in this work shows unchanged resistance (**a**), Seebeck coefficient (**b**) and power factor with a statistical analysis (**c**) upon 1,000,000-time bending at a radius of 3 mm, ensuring its extraordinary elastic *B*-ratio of bending radius to bending times (**d**), with a comparison to that of ever-reported flexible devices[2,16–19,33,36,39–46,48–57].

warming[37], of which the atomic rearrangement could facilitate the hot-rolling process at nearby temperatures. Note the ductility of silver sulfide was attributed to the uncleavable slipping of sub-lattice units[31].

The details of the synthesis, characterizations, and property measurements of Ag_2Se, are shown in the Supplementary. When Ag_2Se is heated up to 150 °C, slightly higher than the orthorhombic-cubic phase transition temperature, it becomes very soft for an easy multi-pass rolling with various thickness down to ~30 μm (Fig. S3). Indeed, a 36 μm thick device focused on here shows a safe bending at a radius of 3 mm for at least 1,000,000 times, as further confirmed by the unchanged thermoelectric properties (Figs. S4, 2). This can be understood by the largely enhanced ε_E^{max} of ~0.8% in rolled Ag_2Se foil (Fig. 1b), because it is larger than the needed strain of ~0.6% ($\varepsilon_E^{max} = t/2r_b$ with a bending radius of r_b and a thickness of t)[38]. Since both minimum r_b and safe bending times are critical parameters for measuring the elastic bendability, a factor B of bending radius to bending times ratio for the Ag_2Se device in this work is significantly smaller than those reported (Fig. 2d).

X-ray diffraction (XRD, Fig. S5) results indicate a preferred [013] orientation of Ag_2Se foils after rolling, and the orientation factor $F_{[013]}$ is about 0.5 (Table S2). Scanning electron microscopy (SEM) observations and energy dispersive spectroscopy (EDS) analyses ensure the compositional homogeneity (Fig. S6). Importantly, thermoelectric performance of hot-rolled foils is quite reproducible with nearly isotropic properties[30] (Fig. S7–S8). The existence of dense dislocations and the increase in carrier concentration lead to a decrease in carrier mobility in the rolled Ag_2Se foils, which further result in a comparable resistivity but a lower Seebeck coefficient (thus a lower power factor particularly at $T > 340$ K, Fig. S9).

A low device contact resistance (R_c) is important to realize the full potential of high-performance thermoelectric materials. Silver paste is usually used for thin-device assembly. To further minimize R_c, the silver foil of 0.1 mm thick is used as an electrode in this work, and Au is deposited on both ends of the hot-rolled Ag_2Se foils to ensure ohmic metallic contacts with the electrode. With the excellent machinability of both Ag_2Se and elementary silver, a firm touching is achieved by bolts and nuts (the inset of Fig. 3a). Uniform mechanical pressure on the foil module is ensured by applying small torque deviation of ~0.0185 ± 0.0005 Nm to the bolts (Fig. S10). The internal resistance (R_{in}) for single-leg foil device with the size of 5 × 5 × 0.036 mm^3 was measured by the four-probe technique across the contacts along multiple parallel paths for averaging (Fig. 3a). The resulting interfacial contact resistivity (ρ_c) at both ends are only ~2.0 and ~2.1 mΩ·cm^2, respectively, being significantly lower than those of reported flexible film devices[15,16,18,33,39–47] (Fig. 3b and Table S3). The consistence between the measured total device resistance of 2.7 Ω and the summation of materials (2.4 Ω) and contact components (0.02 Ω × 12 = 0.24 Ω for 12 in total contacts of ~0.02 Ω each), suggests both good accuracy in ρ_c-determination and uniformity in resistance distribution among contacts.

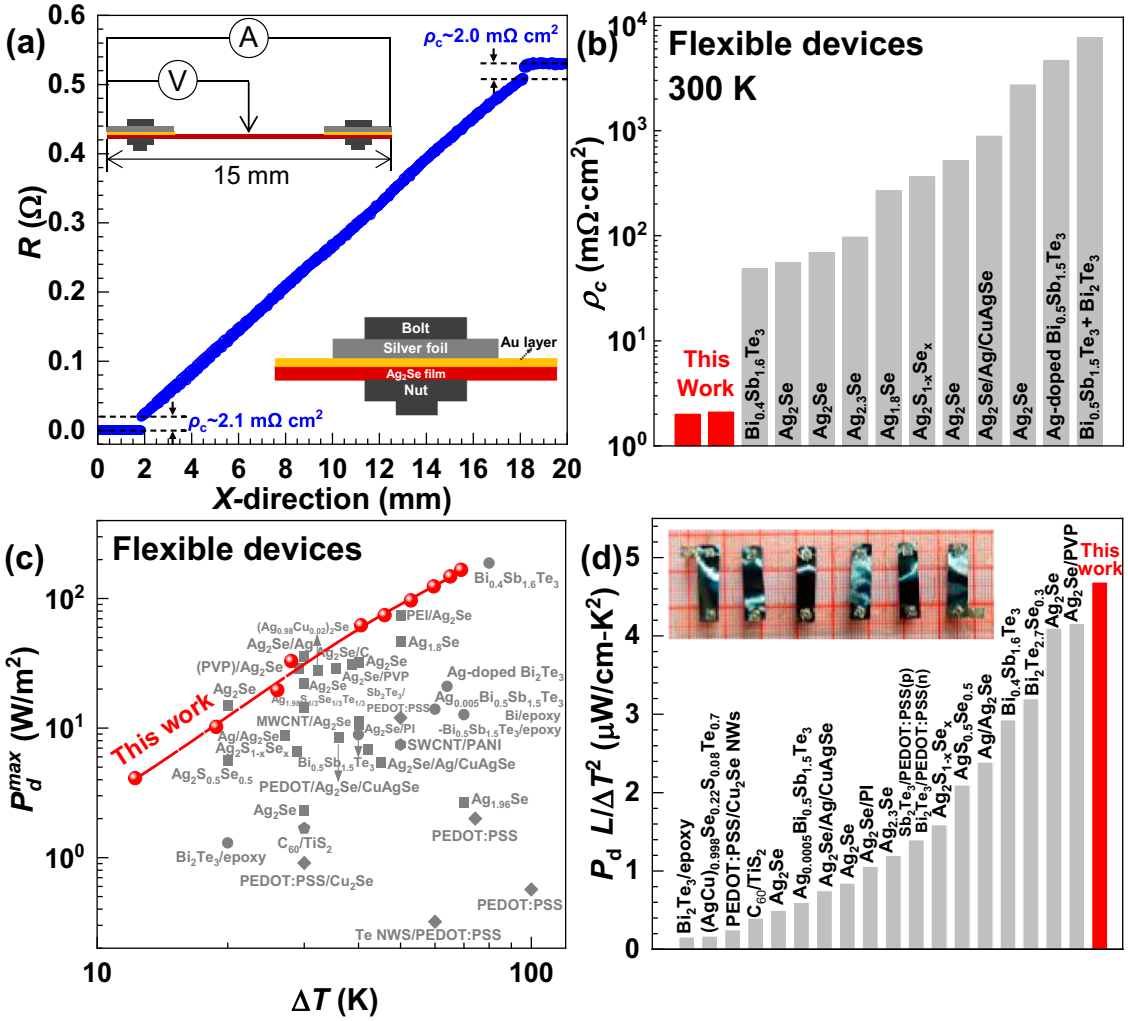

Fig. 3 | Device properties. Scanning resistance (*R*) (**a**) indicates an extremely low interfacial resistivity for flexible film devices of polycrystals (**b**), enabling a superior power density (**c**) and specific power density (**d**), with a comparison to those of ever-reported flexible devices[2,15–19,33,39–47,54–73].

Six n-type Ag_2Se legs of $20 \times 5 \times 0.036$ mm^3 are assembled in this way, paring with copper wires of a positive but quite close to zero Seebeck coefficient, for a device (Fig. S11). Both the output voltage and power at interested temperature gradients are quite comparable to the predictions according to the material properties (Fig. S12). Eventually, a maximum output power (P^{max}) up to 180 μW is reached at ΔT ~ 69 K (Fig. S13), corresponding to a power density (P_d^{max}, power divided by the cross-section area of thermoelectric materials) as high as 167 W/m^2 (Fig. 3c). Moreover, the specific power density ($P_d^{max}L/\Delta T^2$, with L being the leg length) of the device in this work is outstanding (Fig. 3d). Using instead an better performing material, tape-supported single-crystalline Bi_2Te_3-based thin films[48] showed an even higher power density. Limiting the deformations to be elastic and further strengthening its elasticity (Fig. S14) are expected to enable extra robust bendability, performance recoverability, free-standability and mass-producibility. Fig. S15 shows a demonstration of outputting an open-circuit voltage of 4.2 mV under a ΔT of ~8 K.

In summary, the fact that elastic bending fundamentally allows recoverability, in principle offers an additional opportunity of flexibility even in inorganics with rigidity. This work demonstrates in elasticity-strengthened Ag_2Se of an intrinsic large Poisson's ratio, and extrinsic dense dislocations and refined grains, a successful realization of safe bending at a 3 mm radius for at least 1,000,000 times while retaining an extraordinary power output, through a facile hot-rolling technique. This concept is believed to be equally applicable in other materials/devices for topping up functionalities with robust bendability.

Methods

Experimental details of materials and methods are shown in Supplementary Information.

Data availability

All data necessary to understand and assess this manuscript are shown in the main text and the Supporting Information. The data that support the findings of this study are available from the corresponding author upon reasonable request.

Material availability

Requests for materials should be addressed to Yanzhong Pei, Wen Li, and Jun Luo.

References

1. Suarez, F., Nozariasbmarz, A., Vashaee, D. & Öztürk, M. C. Designing thermoelectric generators for self-powered wearable electronics. *Energ. Environ. Sci.* **9**, 2099–2113 (2016).
2. Yang, Q. et al. Flexible thermoelectrics based on ductile semiconductors. *Science* **377**, 854–858 (2022).
3. Goldsmid, H. J. *Introduction to Thermoelectricity*. (Springer, 2009).

4. Pei, Y., Shi, X., LaLonde, A., Wang, H., Chen, L. & Snyder, G. J. Convergence of electronic bands for high performance bulk thermoelectrics. *Nature* **473**, 66–69 (2011).
5. Liu, W. et al. Convergence of conduction bands as a means of enhancing thermoelectric performance of n-Type $Mg_2Si_{1-x}Sn_x$ solid solutions. *Phys. Rev. Lett.* **108**, 166601 (2012).
6. Snyder, G. J. & Toberer, E. S. Complex thermoelectric materials. *Nat. Mater.* **7**, 105–114 (2008).
7. Zhai, R.-S. & Zhu, T.-J. Improved thermoelectric properties of zone-melted p-type bismuth-telluride-based alloys for power generation. *Rare Met.* **41**, 1490–1495 (2022).
8. Liu, K.-J. et al. Entropy engineering in $CaZn_2Sb_2$–$YbMg_2Sb_2$ Zintl alloys for enhanced thermoelectric performance. *Rare Met.* **41**, 2998–3004 (2022).
9. Liu, H.-X., Zhang, X.-Y., Bu, Z.-L., Li, W., Pei, Y.-Z. Thermoelectric properties of $(GeTe)_{1-x}[(Ag_2Te)_{0.4}(Sb_2Te_3)_{0.6}]_x$ alloys. *Rare Metals* **41**, 1–10 (2022).
10. Bubnova, O. et al. Optimization of the thermoelectric figure of merit in the conducting polymer poly(3,4-ethylenedioxythiophene). *Nat. Mater.* **10**, 429–433 (2011).
11. Wan, C. et al. Flexible n-type thermoelectric materials by organic intercalation of layered transition metal dichalcogenide TiS_2. *Nat. Mater.* **14**, 622–627 (2015).
12. Sun, Y. et al. Organic thermoelectric materials and devices based on p- and n-type poly(metal 1,1,2,2-ethenetetrathiolate)s. *Adv. Mater.* **24**, 932–937 (2012).
13. Zhang, Q. et al. Realizing high-performance thermoelectric power generation through grain boundary engineering of skutterudite-based nanocomposites. *Nano Energy* **41**, 501–510 (2017).
14. Lei, Y. et al. Microstructurally tailored thin beta-Ag_2Se films towards commercial flexible thermoelectrics. *Adv. Mater.* **34**, e2104786 (2021).
15. Ding, Y. et al. High performance n-type Ag_2Se film on nylon membrane for flexible thermoelectric power generator. *Nat. Commun.* **10**, 841 (2019).
16. Varghese, T. et al. Flexible thermoelectric devices of ultrahigh power factor by scalable printing and interface engineering. *Adv. Funct. Mater.* **30**, 1905796 (2019).
17. Zheng, Z.-H. et al. Harvesting waste heat with flexible Bi_2Te_3 thermoelectric thin film. *Nat. Sustain.* **6**, 180–191 (2022).
18. Liu, Y. et al. Fully inkjet-printed Ag_2Se flexible thermoelectric devices for sustainable power generation. *Nat. Commun.* **15**, 2141 (2024).
19. Liang, J. et al. Flexible thermoelectrics: from silver chalcogenides to full-inorganic devices. *Energy Environ. Sci.* **12**, 2983–2990 (2019).
20. Deng, T. et al. High thermoelectric power factors in plastic/ductile bulk $SnSe_2$-based crystals. *Adv. Mater.* **36**, 2304219 (2024).
21. Chen, H. et al. High-entropy cubic pseudo-ternary Ag_2(S, Se, Te) materials with excellent ductility and thermoelectric performance. *Adv. Energy Mater.* **14**, 2303473 (2024).
22. Wei, T.-R. et al. Exceptional plasticity in the bulk single-crystalline van der Waals semiconductor InSe. *Science* **369**, 542–545 (2020).
23. Ohashi, T. *Mathematical Modeling of Dislocation Behavior and Its Application to Crystal Plasticity Analysis*. Springer Nature (2023).
24. Valiev, R. Nanostructuring of metals by severe plastic deformation for advanced properties. *Nat. Mater.* **3**, 511–516 (2004).
25. Yoshida, S., Bhattacharjee, T., Bai, Y. & Tsuji, N. Friction stress and Hall-Petch relationship in CoCrNi equi-atomic medium entropy alloy processed by severe plastic deformation and subsequent annealing. *Scr. Mater.* **134**, 33–36 (2017).
26. Wang, L. et al. Tailoring planar slip to achieve pure metal-like ductility in body-centred-cubic multi-principal element alloys. *Nat. Mater.* **22**, 950–957 (2023).
27. Liu, W. et al. Deformation-induced dynamic precipitation of 14H-LPSO structure and its effect on dynamic recrystallization in hot-extruded Mg-Y-Zn alloys. *Int. J. Plast.* **164**, 103573 (2023).
28. Wu, Y. et al. Twisted-layer boron nitride ceramic with high deformability and strength. *Nature* **626**, 779–784 (2024).
29. Chen, M. W., McCauley, J. W., Dandekar, D. P. & Bourne, N. K. Dynamic plasticity and failure of high-purity alumina under shock loading. *Nat. Mater.* **5**, 614–618 (2006).
30. Jin, M. et al. Investigation on low-temperature thermoelectric properties of Ag_2Se polycrystal fabricated by using Zone-Melting method. *J. Phys. Chem. Lett.* **12**, 8246–8255 (2021).
31. Shi, X. et al. Room-temperature ductile inorganic semiconductor. *Nat. Mater.* **17**, 421–426 (2018).
32. He, S. et al. Semiconductor glass with superior flexibility and high room temperature thermoelectric performance. *Sci. Adv.* **6**, eaaz8423 (2020).
33. Lu, Y. et al. Ultrahigh power factor and flexible silver selenide-based composite film for thermoelectric devices. *Energy Environ. Sci.* **13**, 1240–1249 (2020).
34. Wallis, D., Hansen, L. N., Wilkinson, A. J. & Lebensohn, R. A. Dislocation interactions in olivine control postseismic creep of the upper mantle. *Nat. Commun.* **12**, 3496 (2021).
35. Cordier, P., Demouchy, S., Beausir, B., Taupin, V., Barou, F. & Fressengeas, C. Disclinations provide the missing mechanism for deforming olivine-rich rocks in the mantle. *Nature* **507**, 51–56 (2014).
36. Jin, Q. et al. Flexible layer-structured Bi_2Te_3 thermoelectric on a carbon nanotube scaffold. *Nat. Mater.* **18**, 62–68 (2019).
37. Wei, T. R., Qiu, P., Zhao, K., Shi, X. & Chen, L. Ag_2Q-Based (Q = S, Se, Te) silver chalcogenide thermoelectric materials. *Adv. Mater.* **35**, e2110236 (2023).
38. Peng, J. & Snyder, G. J. A figure of merit for flexibility. *Science* **366**, 690–691 (2019).
39. Wu, M. et al. High thermoelectric performance and ultrahigh flexibility $Ag_2S_{1-x}Se_x$ film on a Nylon membrane. *ACS Appl Mater. Interfaces* **15**, 8415–8423 (2023).
40. Lu, Y. et al. Ultrahigh performance PEDOT/Ag_2Se/CuAgSe composite film for wearable thermoelectric power generators. *Mater. Today Phys.* **14**, 100223 (2020).
41. Lu, Y. et al. Good performance and flexible PEDOT:PSS/Cu_2Se nanowire thermoelectric composite films. *ACS Appl Mater. Interfaces* **11**, 12819–12829 (2019).
42. Shang, H. et al. High-performance Ag-modified $Bi_{0.5}Sb_{1.5}Te_3$ films for the flexible thermoelectric generator. *ACS Appl Mater. Interfaces* **12**, 7358–7365 (2020).
43. Gao, Q. et al. High power factor Ag/Ag_2Se composite films for flexible thermoelectric generators. *ACS Appl Mater. Interfaces* **13**, 14327–14333 (2021).
44. Gao, J. et al. Thermoelectric flexible silver selenide films: compositional and length optimization. *iScience* **23**, 100753 (2020).
45. Hou, S. et al. High performance wearable thermoelectric generators using Ag_2Se films with large carrier mobility. *Nano Energy* **87**, 106223 (2021).
46. Jiang, C. et al. Ultrahigh performance of n-Type Ag_2Se films for flexible thermoelectric power generators. *ACS Appl Mater. Interfaces* **12**, 9646–9655 (2020).
47. Shang, H. et al. $Bi_{0.5}Sb_{1.5}Te_3$-based films for flexible thermoelectric devices. *J. Mater. Chem. A* **8**, 4552–4561 (2020).
48. Lu, Y. et al. Staggered-layer-boosted flexible Bi_2Te_3 films with high thermoelectric performance. *Nat. Nanotechnol.* **18**, 1281–1288 (2023).
49. Wang, L. et al. Exceptional thermoelectric properties of flexible organic-inorganic hybrids with monodispersed and periodic nanophase. *Nat. Commun.* **9**, 3817 (2018).
50. Jiang, C. et al. Ultrahigh performance polyvinylpyrrolidone/Ag_2Se composite thermoelectric film for flexible energy harvesting. *Nano Energy* **80**, 105488 (2021).
51. Gao, J. et al. A novel glass-fiber-aided cold-press method for fabrication of n-type Ag_2Te nanowires thermoelectric film on flexible copy-paper substrate. *J. Mater. Chem. A* **5**, 24740–24748 (2017).

52. Wu, B., Guo, Y., Hou, C., Zhang, Q., Li, Y., Wang, H. High-performance flexible thermoelectric devices based on all-inorganic hybrid films for harvesting low-grade heat. *Adv. Funct. Mater.* **29**, 1900304 (2019).
53. Liang, J., Zhang, X. & Wan, C. From brittle to ductile: a scalable and tailorable all-inorganic semiconductor foil through a rolling process toward flexible thermoelectric modules. *ACS Appl. Mater. Interfaces* **14**, 52017–52024 (2022).
54. Lu, Y. et al. Nanoengineering approach toward ultrahigh power factor Ag_2Se/polyvinylpyrrolidone composite film for flexible thermoelectric generator. *Chem. Eng. J.* **485**, 149793 (2024).
55. Zhang, M. et al. Screen printing Ag_2Se/carbon nanocomposite films for flexible thermoelectric applications. *Carbon* **229**, 119480 (2024).
56. Hu, Q. X. et al. Carrier separation boosts thermoelectric performance of flexible n-type Ag_2Se-based films. *Adv. Energy Mater.* **14**, 2401890 (2024).
57. Jia, L. et al. Optimization of power factor for a screen-printed silver selenide-based flexible thermoelectric film by hot pressing. *ACS Appl. Energy Mater.* **7**, 5721–5727 (2024).
58. Madan, D. et al. Dispenser printed circular thermoelectric devices using Bi and $Bi_{0.5}Sb1.5Te_3$. *Appl. Phys. Lett.* **104**, 013902 (2014).
59. Chen, A., Madan, D., Wright, P. K., Evans, J. W. Dispenser-printed planar thick-film thermoelectric energy generators. *J. Micromech. Microeng.* **21**, 104006 (2011).
60. We, J. H., Kim, S. J. & Cho, B. J. Hybrid composite of screen-printed inorganic thermoelectric film and organic conducting polymer for flexible thermoelectric power generator. *Energy* **73**, 506–512 (2014).
61. Rojas, J. P., Conchouso, D., Arevalo, A., Singh, D., Foulds, I. G. & Hussain, M. M. Paper-based origami flexible and foldable thermoelectric nanogenerator. *Nano Energy* **31**, 296–301 (2017).
62. Madan, D. et al. Enhanced performance of dispenser printed MA n-type Bi_2Te_3 composite thermoelectric generators. *ACS Appl. Mater. Interfaces* **4**, 6117–6124 (2012).
63. Du, Y. et al. Multifold enhancement of the output power of flexible thermoelectric generators made from cotton fabrics coated with conducting polymer. *RSC Adv.* **7**, 43737–43742 (2017).
64. Li, C. et al. A simple thermoelectric device based on inorganic/organic composite thin film for energy harvesting. *Chem. Eng. J.* **320**, 201–210 (2017).
65. Li, P. et al. Facile green strategy for improving thermoelectric performance of carbon nanotube/polyaniline composites by ethanol treatment. *Compos. Sci. Technol.* **189**, 108023 (2020).
66. Hokazono, M., Anno, H. & Toshima, N. Thermoelectric properties and thermal stability of PEDOT:PSS films on a polyimide substrate and application in flexible energy conversion devices. *J. Electron. Mater.* **43**, 2196–2201 (2014).
67. Wang, L. et al. Solution-printable fullerene/TiS_2 organic/inorganic hybrids for high-performance flexible n-type thermoelectrics. *Energy Environ. Sci.* **11**, 1307–1317 (2018).
68. Yang, C. et al. Transparent flexible thermoelectric material based on non-toxic earth-abundant p-type copper iodide thin film. *Nat. Commun.* **8**, 16076 (2017).
69. Yang, D. et al. Flexible power generators by Ag_2Se thin films with record-high thermoelectric performance. *Nat. Commun.* **15**, 923 (2024).
70. Dun, C., Kuang, W., Kempf, N., Saeidi-Javash, M., Singh, D. J. & Zhang, Y. 3D printing of solution-processable 2D nanoplates and 1D nanorods for flexible thermoelectrics with ultrahigh power factor at low-medium temperatures. *Adv. Sci.* **6**, 1901788 (2019).
71. Liu, Y. et al. Largely enhanced thermoelectric performance of flexible Ag_2Se film by cationic doping and dual-phase engineering. *ACS Appl. Mater. Interfaces* **16**, 26417–26427 (2024).
72. Kumar, S., Battabyal, M., Sethupathi, K. & Satapathy, D. K. High-performance printed Ag_2Se/PI flexible thermoelectric film for powering wearable electronics. *ACS Appl. Mater. Interfaces* **16**, 40848–40857 (2024).
73. Chen, H. et al. High-entropy cubic pseudo-ternary Ag_2(S, Se, Te) materials with excellent ductility and thermoelectric performance. *Adv. Energy Mater.* **14**, 2303473 (2024).

Acknowledgements

This work is supported by the National Key Research and Development Program of China (2023YFB3809400), the National Natural Science Foundation of China (Grant No. T2125008, 92163203, 52371234 and 92263108), the Innovation Program of Shanghai Municipal Education Commission (2021-01-07-00-07-E00096) and the Hong Kong, Macao and Taiwan Science and Technology Cooperation Project for Science and Technology Innovation Plan of Shanghai (23520760600). We thank Dr. Shuai Chen from Oxford Instruments Technology (Shanghai) Co. Limited for the EBSD analyses.

Author contributions

Y.Z.P., W.L., and J.L. conceived this study and led the project. W.J.D., X.Y.S., and Y.X.H. carried out the experiments. M.J., Z.W.C., and E.C.M. carried out part of the characterizations. W.J.D. and W.L. wrote the manuscript. All authors commented on the manuscript.

Competing interests

The authors declare no competing interests.

Additional information

Supplementary information The online version contains supplementary material available at https://doi.org/10.1038/s41467-024-54084-6.

Correspondence and requests for materials should be addressed to Jun Luo, Wen Li or Yanzhong Pei.

Peer review information *Nature Communications* thanks the anonymous reviewers for their contribution to the peer review of this work. A peer review file is available.